NUCLEAR SCIENCE AND TECHNIQUES **25**, 060101 (2014)

X-band deflecting cavity design for ultra-short bunch length measurement of SXFEL at SINAP*

TAN Jian-Hao (谭建豪),[1,2] GU Qiang (顾强),[1] FANG Wen-Cheng (方文程),[1]
TONG De-Chun (童德春),[3] and ZHAO Zhen-Tang (赵振堂)[1,4,†]

[1]*Shanghai Institute of Applied Physics, Chinese Academy of Sciences, Shanghai 201800, China*
[2]*University of Chinese Academy of Sciences, Beijing 100049, China*
[3]*Department of Engineering Physics, Tsinghua University, Beijing 100084, China*
[4]*Shanghai Key Laboratory of Cryogenics & Superconducting RF Technology, Shanghai 201800, China*

(Received June 20, 2013; accepted in revised form August 27, 2014; published online December 20, 2014)

For developing the X-ray Free Electron Lasers test facility (SXFEL) at Shanghai Institute of Applied Physics, Chinese Academy of Sciences (SINAP), ultra-short bunch is the crucial requirement for excellent lasing performance. It is a big challenge for deflecting cavity to measure the length of ultra-short bunch, and higher deflecting gradient is required for higher measurement resolution. X-band travelling wave deflecting structure has features of higher deflecting voltage and compact structure, which has good performance at ultra-short bunch length measurement. In this paper, a new X-band deflecting structure is designed to operate in HEM11-2$\pi/3$ mode. For suppressing the polarization of deflecting plane of the HEM11 mode, two symmetrical caves are added on the cavity wall to separate two polarized modes.

Keywords: HEM11, Bunch length, Dipole mode, Polarization, Time domain

DOI: 10.13538/j.1001-8042/nst.25.060101

I. INTRODUCTION

The 840 MeV linac-based X-ray free electron lasers test facility (SXFEL) will be built at Zhangjiang campus of Shanghai Institute of Applied Physics (SINAP), where Shanghai Synchrotron Radiation Facility (SSRF) is situated [1]. SXFEL will be a compact coherent X-ray source, and its total length is about 300 meters. This facility will generate electron beams of low emittance and short bunch length, which is about 2.5 µm and 120 µm, respectively. For ultra-short electron bunch length measurement, a standard method as used at LCLS (Linac Coherent Light Source) with a new X-band deflecting structure, using the principle of bunch length measurement works and stream camera for electrons, but the deflector is capable of resolving bunch length of 10 fs. The deflecting cavity operates in a dipole mode, for suppressing polarization of deflection plane in HEM11 mode, with two symmetrical caves added on the cavity wall [2]. A novel transverse RF deflecting structure is introduced to diagnose longitudinal structure of the bunch (Fig. 1).

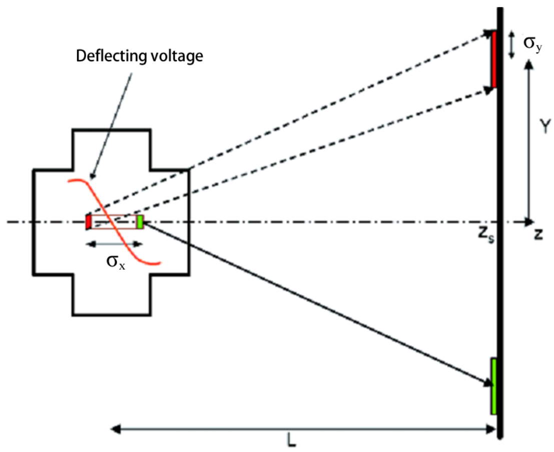

Fig. 1. (Color online) Schematics of an RF deflector.

II. DEMANDED PERFORMANCE

In SXFEL, the deflecting structure will be located at 3 m after the last bunch compressor at 0.84 GeV, with an emittance of 2.5 µm and bunch length of 120 µm. The deflecting voltage V_{T} is given by

$$eV_{\mathrm{T}} = \frac{E\lambda/c}{2\pi\sigma_t R_{34}}\sqrt{\sigma_y^2 - \sigma_{y,0}^2}, \tag{1}$$

where V_{T} is the transverse deflecting voltage, and E is the electron energy, σ_t is the longitudinal beam size on the time scale, λ is the RF wavelength, R_{34} is the element of the transport matrix, and σ_y and $\sigma_{y,0}$ is the vertical beam size on the screen when the deflector is on and off. When a length of drift space between the deflector and screen is taken into consideration, R_{34} is the drift space length D. For a complicated system, such as a focusing system composed of several quadrupoles, R_{34} can be obtained by multiplying the transport matrices. Generally, $R_{34} = (\beta_{\mathrm{d}}\beta_{\mathrm{s}})^{1/2}\sin\psi$, where β_{d} and β_{s} are the beta function at the deflector and screen, respectively, ψ is the phase shift between the beta oscillation at the deflector and screen on deflection plane. For deflecting structure, the resolution is an important conception defined as $\Delta_t = E\sigma_{y,0}(\omega V_{\mathrm{def}} R_{34})$, where $\sigma_{y,0}$ can be stated by $(\varepsilon_N, \varepsilon_y/\gamma)^{1/2}$ [3]. Higher time resolution can be acquired under higher frequency and voltage. Also, lower energy and emittance, and larger drift space or beta function at the

---

* Supported by the Knowledge Innovation Project of the Chinese Academy of Sciences (No. 455011061)
† Corresponding author, zhaozhentang@sinap.ac.cn

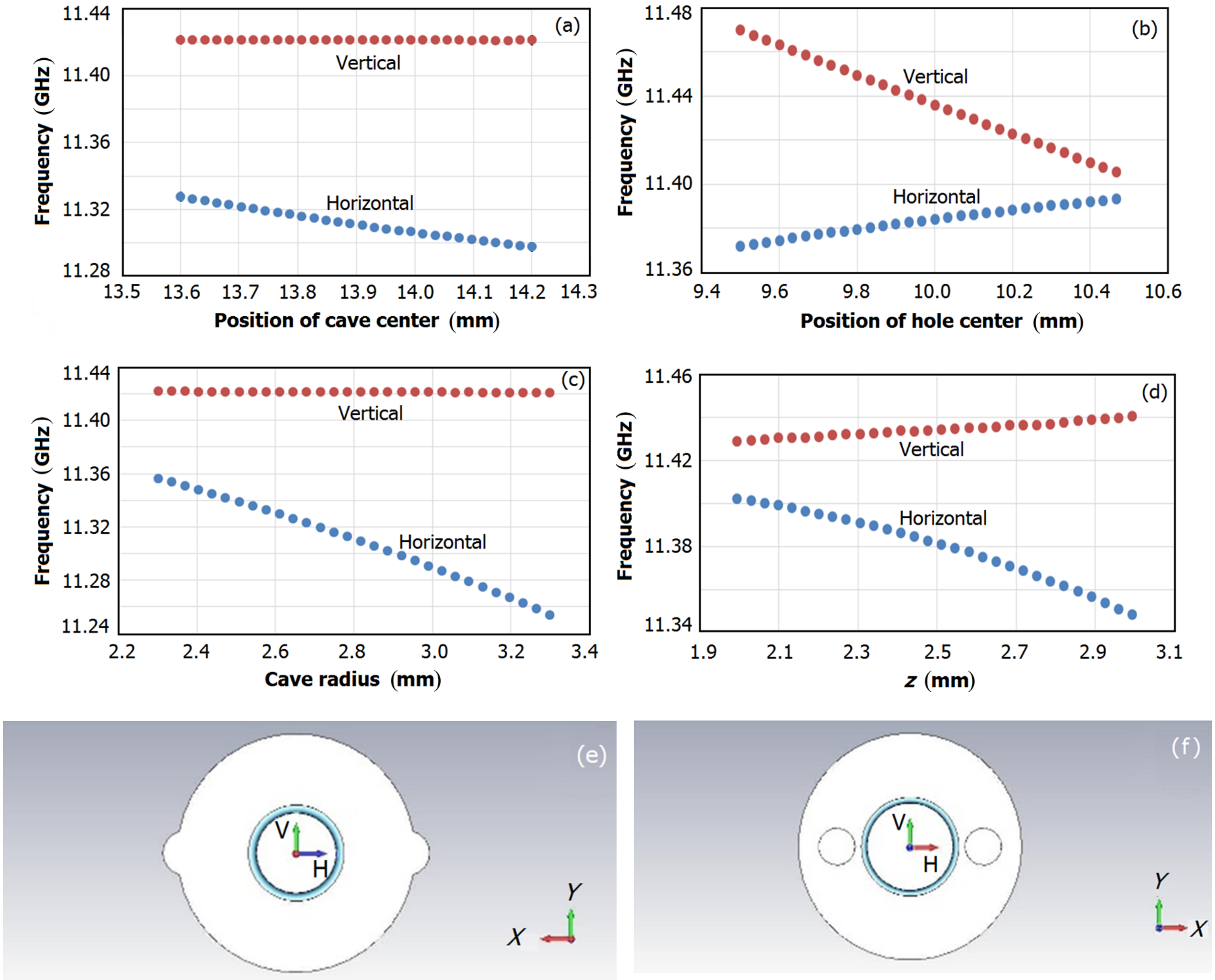

Fig. 2. (Color online) Simulation results of the effects on frequency by added variation of caves center (a), caves radius (c), holes center (b), and holes radius (d).

deflector are preferred. Considering the costs, a lower power-feed structure program is proposed due to enough space. In addition, a compact facility needs smaller, shorter and higher gradient structure. Therefore, an X-band disk-loaded waveguide structure is the best choice. Table 1 lists specifications of the X-band deflector for SXFEL, which will work at traveling wave state and HEM11 mode. Performance of a deflector is determined by transverse shunt impedance, group velocity and attenuation factor, as described by Eq. (2):

$$V_{\mathrm{T}}^2 = \frac{2}{\tau}(1-e^{-\tau})P_0 R_s L, \tag{2}$$

where τ is the attenuate coefficient, P_0 is the input power, R_s is the transverse shunt impedance and L is the total length of the structure.

According to performance of the SXFEL, a deflector with temporal time resolution of 20 fs is needed. Considering the room for beam deflection and drift, and the 10 MW power limit to save expense, a high transverse shunt impedance deflecting structure shall be an optimum scheme.

TABLE 1. Specifications of x-band deflector for SXFEL

Structure type	Constant impedance
Operating frequency (GHz)	11.424
Operating mode	Disk-loaded waveguide $2\pi/3$
Energy (GeV)	0.84
Bunch length (µm)	120
Bunch size (y) (µm)	60
Drift space (m)	5
Desired temporal resolution (fs)	20
Deflecting voltage (MV)	12–35
Input power (MW)	< 20
Total length L (m)	< 1

III. DESIGN OF REGULAR CELLS

The HEM11 mode in an axis-symmetric structure degenerates in twofold, and it leads to the rotation of deflection plane or polarization plane. This brings inconvenience when deflecting cavity is used to measure the beam size. To solve

the degeneracy and prevent rotation of the deflection plane, SLAC proposed to have two symmetrical holes on the iris which called LOLA [4], and two symmetric caves were added on the cavity wall [5]. At Spring-8, a racetrack structure was designed for cancelling the degeneracy of the HEM11 mode [6]. Then, frequency of the degenerate modes has a mode gap that depends on the degree of the symmetries-broken.

A. Selection of scheme

To facilitate the fabrication and tuning processes, the influence on frequency by different designs was simulated. The results are shown in Fig. 2.

From Fig. 2 one sees that the caves structure is superior to holes structure. The caves center position and cave radius have little effect in the vertical direction, but affect the frequency significantly in horizontal direction (the caves or holes were added on the horizontal direction in the simulation). So, the SLAC caves structure is used in the deflector design.

The dispersion diagrams of HEM11 mode change from forward to backward when a/b varies from large to small [7], and the dispersion is a hybrid of TM11 and TE11 mode. Then, the single chain of coupled circuit model is not suitable, and the double chain of circuit model is needed, which means the field in each cell is a combination of a TM11 mode and a TE11 mode. The details are presented in Ref. [8], and the final expression is Eq. (3):

$$\cos\theta = \frac{-k_1k_2 - \left(1-\frac{f_1^2}{f^2}\right)\left(1-\frac{f_2^2}{f^2}\right)}{\left(1-\frac{f_1^2}{f^2}\right)k_2 + \left(1-\frac{f_2^2}{f^2}\right)k_1}, \tag{3}$$

where k is the couple coefficient and f is regular frequency, with the subscripts 1 and 2 representing TM11 and TE11, respectively. The results with double chain of circuit model were calculated, and single chain of circuit model, for comparison, was calculates, too. As shown in Fig. 3, the CST simulation results of double chain of circuits model are consistent with the dispersion curve of HEM11 mode.

The definition of group velocity and attenuation factor are $V_{\rm g} = {\rm d}\omega/{\rm d}\beta$ and $\alpha = \pi f/(QV_{\rm g})$. Taking advantage of the dispersion curve, it is easy to calculate the group velocity, and the attenuation factor can be fitted when the quality factor (Q) of the cell is clear. It is fortunate that the Q value is given by the template post processing of CST. The group velocity indicates the velocity of power flow which determines the scale of feed-in power, and high power flow represents the high power accumulation which leads to high breakdown rates. Therefore, the cavity with low group velocity is a more appropriate choice than high group velocity for high gradient structure. To reduce the feed-in power, the cells with high shunt impedance are preferred. In accelerating structures, the longitudinal shunt impedance R is defined as

$$R = E_z^2/(-{\rm d}p/{\rm d}z), \tag{4}$$

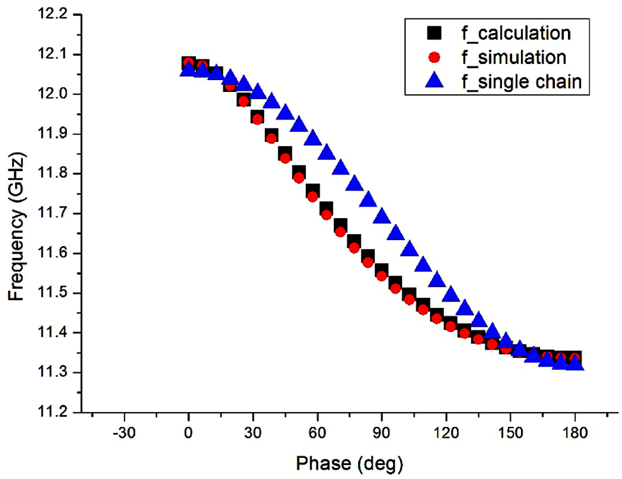

Fig. 3. (Color online) Single chain and double chain of circuit model applied to HEM11 mode.

where E_z means the electric field on-axis along z.

For deflecting structure, the transverse shunt impedance R_s is more useful, which is defined as [9]

$$R_s = [(\partial E_z/\partial r)/k]^2/(-{\rm d}p/{\rm d}z), \tag{5}$$

where z and r is longitudinal and transverse axis, respectively; E_z is the electric field amplitude for the dipole mode with angular frequency ω; and P is the RF power as function of z. Using the simulation codes for electromagnetic field in RF structures, the transverse shunt impedance can be calculated from

$$R_s = c^2QV_z^2/(\omega^3r_0^2UL), \tag{6}$$

where Q, U and L are quality factor, stored energy and length of the cavity, respectively; V_z is the integral of E_z along the cavity length; and r_0 is the off-axis position. The transverse size of bunch is in several micrometers generally, which means bunch deflected by deflector located in the center of cavity ($r_0 = 0$), and the gradient of E_z is linear when r_0 near cavity center. For brief description, the transverse shunt impedance on the axis is the transverse shunt impedance of the cavity.

B. Simulation of regular cells

Now that the caves type is chosen for the X-band deflector design, and the performance is proposed, the regular cells are simulated and the key parameters are calculated to evaluate property of the cells. For meeting the demanded performance, the initial scheme is to decrease the feed-in power as low as possible. Therefore, transverse shunt impedance is major parameter to optimize.

As mentioned above, the a/b ratio has an impact on power flow direction. With a decreasing a/b, the group velocity changes from positive to negative, which means the power

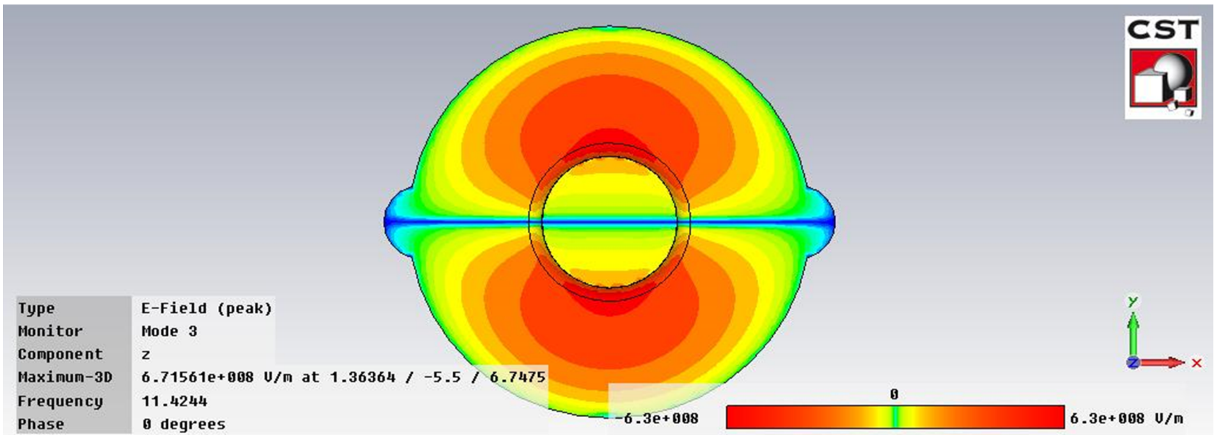

Fig. 4. (Color online) Electric field in the regular cell.

TABLE 2. Specifications in HEM11 mode at $a/b = 0.37 \sim 0.23$

$a(a/b)$ (mm)	Group velocity (%c)	Transverse shunt impedance (MΩ/m)	Quality factor	Attenuation factor (m^{-1})
5.5(0.37)	−2.46	38.35	6662	0.730
5.2(0.35)	−2.98	42.24	6622	0.606
5.0(0.34)	−3.17	46.04	6778	0.564
4.5(0.30)	−3.18	54.09	6924	0.543
4.0(0.26)	−2.62	61.53	7072	0.646
3.5(0.23)	−2.02	68.81	7821	0.757

flow and the beam are of opposite directions. Also, the scale of $2a$ has an effect on transverse shunt impedance, group velocity, and attenuation factor. Therefore, at different a/b, they are calculated at 11.424 GHz, and the results are given in Table 2. To get deflection gradient as high as possible, the iris radius shall be as small as possible. However, the short range wakefield, to some extent, is dominated by the diameter of iris aperture $2a$, which can induce a strong effect on the emittance dilution and energy distribution of the bunch.

The relationship of short range wakefiled (SRW) and iris radius a is given by (in mm) [10]

$$\begin{aligned} &\text{Longitudinal}\quad \text{SRW} \\ &W(s) = \frac{Z_0 c}{\pi a^2} e^{-1.16 s^{0.55}}, \\ &\text{Transverse}\quad \text{SRW} \\ &W(s) = \frac{2 Z_0 c}{\pi a^4}\left(1 - e^{-0.89 s^{0.87}}\right). \end{aligned} \tag{7}$$

where s is the distance from the head of the bunch and $Z_0 = 377\,\Omega$.

By an overall consideration, especially the beam quality and transverse shunt impedance for reducing the feed-in power, as a compromise, the radius of beam hole is 4 mm.

Electric field on the iris is simulated in HEM11 mode. The results are plotted in Fig. 4. As shown in Table 3, for the iris thickness t from 2.2 mm to 1.8 mm, the group velocity keeps almost the same, the transverse shunt impedance and quality factor increase a little, but the attenuation has a 8.6% decrease. This is a good degree of improvement, the iris thickness of 1.8 mm is a reasonable choice.

TABLE 3. Specifications in HEM11 mode at $t = 2.2 \sim 1.8$ mm

t (mm)	Transverse shunt impedance (MΩ/m)	Group velocity (%c)	Q value	Attenuation factor (m^{-1})
2.2	45.62	3.17	6345	0.595
2.0	49.07	3.17	6778	0.557
1.8	50.31	3.16	6965	0.544

TABLE 4. Initial scheme of deflectors for 20-fs temporal resolution

Structure type	Constant impedance
Operating frequency (GHz)	11.424
Operating mode	Disk-loaded waveguide $2\pi/3$
Total length L (mm)	47 cells+2 couplers (440)
Resolution (fs)	20
Deflecting voltage (MV)	7
Input power (MW)	5
Group velocity V_g (%c)	−2.62
Filling time t_F (ns)	51

With the chosen parameters of the cells and the available beam parameters and performance of the cells, the feed-in power and the length of the structure can be calculated. The deflector length can be estimated by Eq. (2). A 0.5-m long deflector is utilized to measure the bunch length, by taking into account the power utilization efficiency, the space to install the deflector and the input power level. Therefore, less than 50 regular cells are needed [11]. The initial scheme of the regular cells are listed in Table 4.

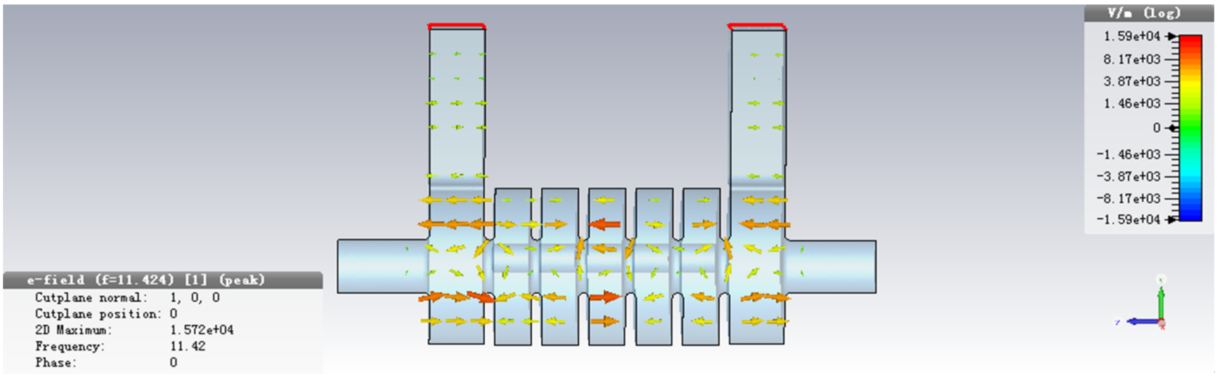

Fig. 5. (Color online) Single-feed standard coupler models and field distribution.

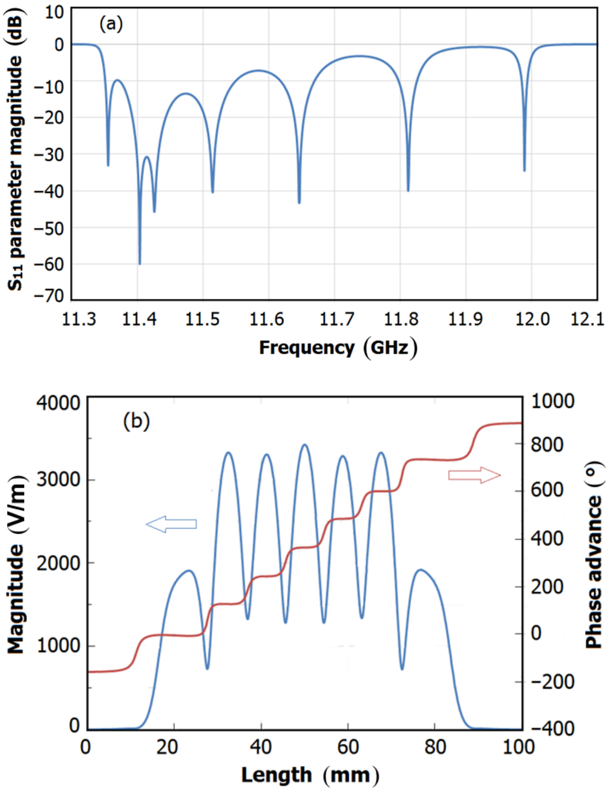

Fig. 6. (Color online) The results of S_{11} parameter (a), and Z component of electric field and phase distribution (b).

C. Design of coupler

The designed regular cells provide outstanding performance, but an RF coupler is an important microwave structure to feed power into the cavity and keep its high efficiency. The primary mission of couplers is feed power as much as possible from the klystron to the regular cells. One feed port is enough for a standing wave structure, while two couplers are needed for a travelling wave structure. A simulation by CST frequency domain solver was performed, and the phase advance and reflect coefficient were calculated by time domain method [12], for a suitable type of coupler among the mode launcher, waveguide and standard couplers.

Generally, mode launcher and waveguide couplers are dual-feed coupler. The affection of multipole field components is negligible in deflecting cavity [13], but with transverse and longitudinal compactness, standard coupler is suitable for deflecting cavity. Considering the total length and the efficiency, standard coupler is the best choice. A single-feed standard coupler is shown in Fig. 5.

The simulation was done with five identical regular cells and two identical (input/output) couplers owing to constant impedance structure. The results are illustrated in Fig. 6.

Due to the electric field along z axis is null, the off-axis electric field was taken into consideration. The simulation results show that the field in the coupler is slightly lower than the cavity, with periodic structures. These seem to show that the couplers have been matched. The structure tuning includes two parts: the cavity and the couplers. It shall be ensured that the phase shift of the cavity is corresponding to the operating mode and the reflection coefficient of the coupler is lower than 0.03 to eliminate the standing wave in the cavity. The time domain methods in Eq. (8) can check whether the couplers are matched or not.

$$\begin{aligned}
F^{\pm}(z) &= \frac{E_c(z+p)}{E_c(z)}, \\
\sum(z) &= F^{+}(z) + F^{-}(z), \\
\Delta(z) &= F^{+}(z) - F^{-}(z), \\
\cos\varphi &= \frac{1}{2}\sum(z), \\
Re^{2j\Phi} &= \frac{2\sin\varphi + j\Delta(z)}{2\sin\varphi - j\Delta(z)},
\end{aligned} \tag{8}$$

where $E(z)$, φ and R are the distribution of electric field along z, regular cell phase advance and reflection coefficient, respectively. Fig. 7 shows the calculation results, which indicate that the couplers are matched and the phase advance is 120°. It is obvious that the two values $\cos\varphi$ and R are indeed constant over the allowed range, and φ is corresponding to phase shift $2\pi/3$. It suggests that the regular cells operate at the frequency we wanted. The reflection coefficient

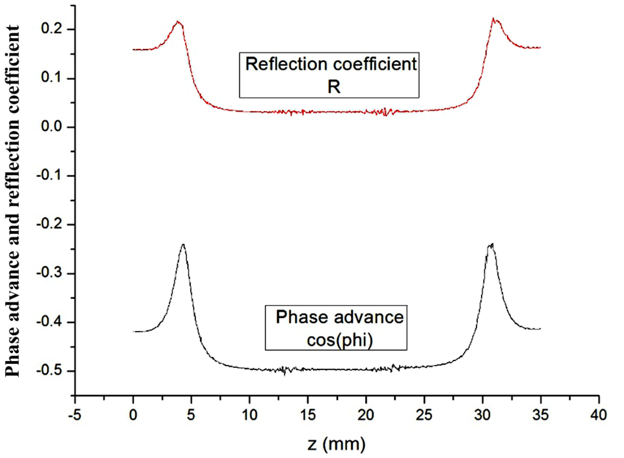

Fig. 7. (Color online) Reflection coefficient and phase advance (matched).

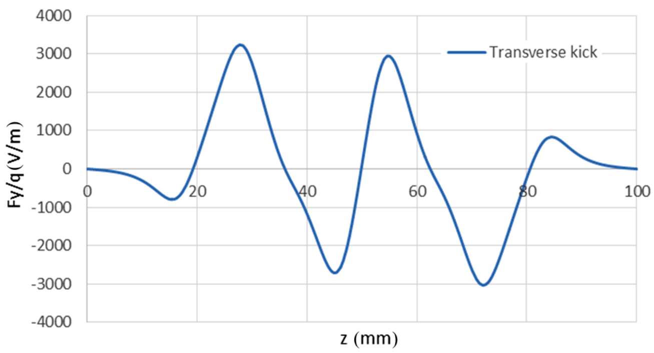

Fig. 8. (Color online) Transverse electric fields seen by beam.

R demonstrates that the couplers have satisfied the matching condition.

The dipole kick can be derived from the CST codes. The total transverse Lorentz force can be expressed as:

$$F_{\text{kick}} = qE_y(z)\cos\Psi, \tag{9}$$

where E_y and Ψ are transverse electric fields which cause beam deflection and initial phase, respectively. The in-phase and forces due to transverse electric field that act on electron traveling at the speed of light are plotted in Fig. 8. It shows that the transverse fields in the single feed coupler and the fields in the couplers are lower than cavities. This proves that the single feed couplers are suited for travelling wave deflecting cavities.

IV. CONCLUSION

A transverse travelling wave deflecting structure of a disk-loaded waveguide has been designed and optimized for SXFEL at SINAP, with two caves in horizontal orientation to stable the polarization plane. The transverse shunt impedance could be up to 60 MΩ/m, therefore a 47-cell long deflecting structure fed with an RF power of 5 MW generates a total deflecting voltage of 7 MV, then we can measure the bunch length with a time resolution of 20 fs by using this high gradient deflector. For higher energy or getting higher resolution, improving the fed power could meet the requirement. In the next step, a prototype of the X-band deflecting cavity will be manufactured, and its beam test will be carried out at Shanghai deep ultraviolet free-electron laser (SDUV-FEL) [14], and the final prototype will be installed on SXFEL in the near future.

[1] Jiang M, Yang X, Xu H J, *et al*. Chin Sci Bull, 2009, **54**: 4171–4181.
[2] Wang J W, Tantawi S, Park M. THP075: X-band traveling wave rf deflector structures, Proceedings of LINAC08, Victoria, BC, Canada, 2008, 966–968.
[3] Emma P, Frisch J, Krejcik P. A transverse rf deflecting structure for bunch length and phase space diagnostics, SLAC, LCLS-TN-00-12, Aug. 29, 2000.
[4] Akre R, Bentson L, Emma P, *et al*. Bunch length measurements using a transverse RF deflecting structure in the SLAC LINAC, Proceedings of EPAC 2002, Paris, France, 2002, 1882–1884.
[5] Wang J W. X-band deflectors development at SLAC. Dec. 2008.
[6] Ego H and Otake Y. TUPC023: Design of the transverse c-band deflecting structure for measurement of bunch length in X-FEL, Proceeding of EPAC2008, Genoa, Italy, 2008, 1098-1100.
[7] Wang J W and Loew G A. HEM11 modes revisited. SLAC-PUB-5321, Sep. 1990.
[8] Bane K L F, Gluckstern R, Holtkamp N. The coupled dipole modes of the NLC accelerator structure. SLAC-PUB-5766, Mar. 1992(A).
[9] Larsen R R and Loew G. The definition and measurement of the shunt impedance of an rf particle deflector. SLAC-tn-62-057, Oct. 1962.
[10] Bane K, Timm M, Weiland T. The short-range wakefields in the SBLC linac. DESY Report, DESY M-97-02, Hamburg, Germany, 1997.
[11] Zhao Z T, Chen S Y, Yu L H, *et al*. THPC053: Shanghai soft x-ray free electron laser test facility, Proceedings of IPAC2011, San Sebastian, Spain, 2011, 3011-3013.
[12] Kroll N M, Ng C K, Vier D C. Applications of time domain simulation to coupler design for periodic structures. SLAC-PUB-8614, Sep. 2000, physics/0008201.
[13] Ambattu P K, Burt G, Grudiev A, *et al*. Phys Rev ST Accel Beams, 2013, **16**: 062001.
[14] Deng H X. Nucl Sci Tech, 2014, **25**: 010101.